

Dynamic Modeling and Simulation of Catalytic Naphtha Reforming

H.M.Arani¹, S.Shokri², M.Shirvani³

Abstract—In this paper, according to the recent progresses in naphtha reforming technology, dynamic modeling of catalytic naphtha reforming process is studied. The dynamic model is composed of the reforming reaction model, the heat exchanger model, furnace model, which together, are capable to capture the major dynamics that occur in this process system. Kinetic modeling of the reactions of the fixed bed reactors connected in series form the most significant part of the overall simulation effort. MATLAB software in SIMULINK mode is used for dynamic simulation. Hougen-Watson Langmuir-Hinshelwood type reaction rate expressions are used to represent rate of each reaction. The results show models are in fair agreement with the actual operating data.

Index Terms—Catalytic reforming, Dynamic modeling, Simulation, Naphtha

I. INTRODUCTION

Catalytic naphtha reforming is an important process for producing high octane gasoline, aromatic feedstock and hydrogen in petroleum-refining and petrochemical industries.

Advanced process control and process optimization strategies are important to be considered in catalytic reforming of naphtha due to its impacts on refineries profit. These are achieved mostly via a reliable mathematical dynamic model.

The catalytic reforming process came into operation in refineries in the late 1940s. The reforming of naphtha feed stocks over platinum catalysts was pioneered by Universal Oil Products (UOP), with the plat forming process introduced in 1947.

Concerning the kinetic modeling of the naphtha processes Smith [1] firstly proposed a four lumps model by considering naphtha as being composed of naphthenes, paraffins, aromatics and light hydrocarbons (<C₅), lumps with average carbon number properties in 1959. However, it is not much precise because of its limited lumps. Kmak [2] developed a detailed model (Exxon model) including twenty-two lumps, which was refined by Froment [3] who developed a more detailed twenty-eight lumps model with 81 reactions. Ramage [4] developed the Mobile thirteen lumps model that considered the adsorption of chemical lumps on the catalyst

surface.

More recently Jorge [5] presented a twenty-four lumps model with 71 reactions and Taskar [6] proposed a more detailed thirty-five lumps model used for the optimization of semi-regenerative naphtha catalytic reformers. Generally speaking, detailed models are theoretically sound but quite complicated, consequently difficult for application because of very complex lumping scheme and parameter estimation to maintain a good balance between kinetics, simplicity and applicability of the model [7].

On the other hand, dynamic modeling was performed by Yongyou et al. [15] by a 17 lumps kinetic model and solution was performed after linearization. Actually, very limited attempt on dynamic simulation of this process have been appeared in the literature. A modeling and dynamic simulation on the catalytic reforming process was carried out by Ansari [16] using Smith's kinetic scheme.

A. Process Description

Catalytic naphtha reforming contains three reactors in series, as shown in Fig. 1. It is generally carried out in three/four fixed or moving bed reformers. The catalyst used in reformer is commonly a bifunctional bimetallic catalyst such as Pt-Re/Al₂O₃, providing the metal function and the acid function. The product stream from the first reactor after preheating enters the second reactor and similarly the product stream from the second reactor after preheating enters the third one. Thus, the reactor feeds are raised to the proper temperature by heaters located before the reactors, since the reactions are endothermic. The product stream from the final reactor enters a separator wherein hydrogen rich gas stream is separated from the products which is then recycled back and mixed with the first reactor fresh feed. Reactors are of different sizes, with the smallest one located in the first stage and the largest one in the last. Temperature profile of the reactors is shown in Fig. 2.

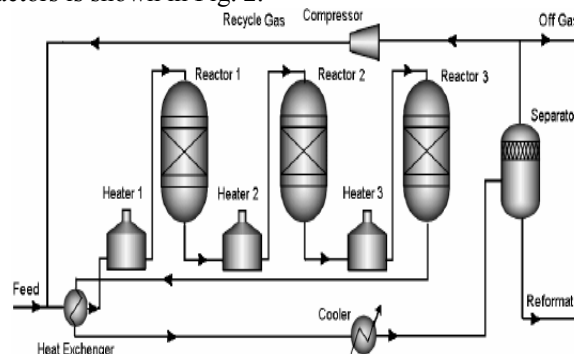


Figure 1. Process flow scheme of the catalytic naphtha reformer

^{1,2} Research Institute of Petroleum Industry (RIPI), West Blvd. Azadi Sport Complex, Tehran, Iran

³ Assistant Professor, School of Chem. Eng., Iran Univ. Sci. Tehran., Iran
Corresponding author: Tel.: +982148252503; fax: +982144739713
E-mail address: Shokris@ripi.ir

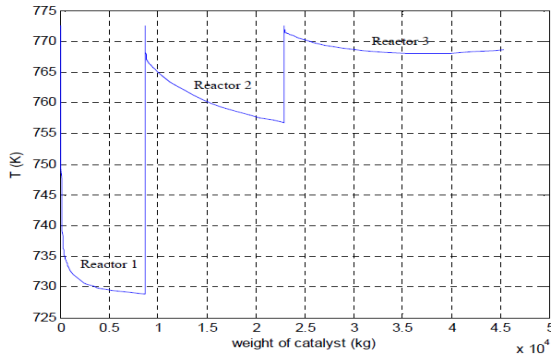


Figure 2. Temperature distribution in reactors length

II. DYNAMIC MODEL

There are a number of different methods for modeling the catalytic reforming process, and the main idea behind all of them is to determine the operating conditions of the reforming unit and to predict the yield of reformate and the temperature profile accurately.

A model must predict the behavior not only within the reactor, but in the auxiliary areas of the unit as well. It should also consider the complex nature of the process and the reactions which take place during the process of reforming.

A. Reaction Kinetic Model

Reactions of catalytic naphtha reforming are elementary and Hougen-Watson Langmuir- Hinshelwood type of reaction rate expressions are used to describe the rate of each reaction.

Rate expressions of this type explicitly account for the interaction of chemical species with catalyst and contain denominators in which characteristic terms of adsorption of reacting species are presented. The reaction rate coefficients obey the Arrhenius law. All reaction rate equations are shown in Table 1.

TABLE 1: REACTION RATE EQUATIONS

| Reactions | Equations |
|---------------------------------|-------------------------------------------------------------------------------------------------------|
| Isomerization of paraffins | $r = k_e \frac{-E}{RT} \frac{(P_p - P_{np} / K_{ip \leftrightarrow np})}{(P_{H_2} \Gamma)}$ |
| Dehydrocyclization of paraffins | $r = k_e \frac{-E}{RT} \frac{(P_{np} - P_N P_{H_2} / K_{np \leftrightarrow N})}{(P_{H_2} \Gamma)}$ |
| Dehydrogenation of naphthenes | $r = k_e \frac{-E}{RT} \frac{(P_{np} - P_A P_{H_2}^3 / K_{N \leftrightarrow A})}{(P_{H_2} \theta)^2}$ |
| Cracking of paraffins | $r = k_e \frac{-E}{RT} \frac{P_p}{\Gamma}$ |
| Hydrodealkylation of aromatics | $r = k_e \frac{-E}{RT} \frac{P_A}{\Gamma}$ |

In the above table, adsorption terms for the metal function (θ), and for the acid function (Γ), are defined as follows (Van. Trimpont, Marin and Froment, 1988)

$$\Gamma = (P_{H_2} + 107P_{C_6} + 21.9(P_{ip} + P_{np}) + 659P_N + 0.703P_{H_2} P_A) / P_{H_2}$$

$$\theta = (1 + 0.0027P_N + 8.314 \exp(-11658.6/T) P_N \times 10^{11} / P_{H_2})$$

Where, P_i in the above equations is the partial pressure of the components and T is the temperature. As done by Hu et al. (2003) [9] and Taskar (1996) [6], all constants of adsorption terms were obtained by studying the reforming of C_7 hydrocarbons. Thermodynamics of reactions are considered in another work [10].

B. Reactors Dynamic Model

A dynamic mathematical model with the kinetics described above is developed by assembling the mass and energy balance on the system of reforming reactions. The mass balance provides the variation of the concentrations of the components along the reactors, and the energy balance gives the variation of temperature. Mass and energy balances for each reformer are both nonlinear partial differential equations in space and time. By taking component material balances as well as energy balance on a differential element “ dw ” of catalyst bed the following system of differential equations can be obtained.

Mass balance equations for an element of catalyst weight in a plug flow reactor (proved in appendix A) are:

$$-\frac{dF_i}{dw} + \sum_{j=1}^{n_r} \gamma_{i,j} r_j = \frac{\varepsilon}{\rho_b} \frac{d(c_i)}{dt} \quad (1)$$

Where:

$$y_i = \frac{c_i}{\sum_{i=1}^{n_c} c_i} = \frac{F_i}{\sum_{i=1}^{n_c} F_i} \quad (2)$$

$$F_t = \frac{\dot{m}}{M_{av}} \quad (3)$$

$$M_{av} = \sum_{i=1}^{n_c} y_i M_i \quad (4)$$

$$F_i = y_i F_t \quad (5)$$

The energy balance equation for the reactor shown in Fig. 1 can be written (proved in appendix B) as:

$$\frac{dT}{dt} = \frac{-\left(\sum_{i=1}^{n_c} F_i C_{pi}\right) \frac{dT}{dw} - \sum_{j=1}^{n_r} r_j \left(\sum_{i=1}^{n_c} H_i \gamma_{i,j}\right)}{\left(C_{p\text{cata}} + \frac{\varepsilon}{\rho_b} \sum_{i=1}^{n_c} c_i C_{pi}\right)} \quad (6)$$

Where, n_i is the number of moles of i^{th} lump for element with dw of catalyst weight.

Where,

$$H_i = H_0 + \int_{T_0}^T C_{pi} dT \quad (7)$$

In Hu et al. [9] catalyst heat capacity in the denominator of energy equation was ignored, while this has great influence on dynamic response of reactors.

C. Furnace Model:

Simple model of fired heater furnaces are used here.

In the mathematical model of this system the following assumptions are used:

- 1) Outlet gas temperature from the furnace is equal to tube wall temperature
- 2) The temperature of the tube wall is equivalent over the length of tube
- 3) Variation of gas temperature inside tube is linear

We consider the tubes for heat transfer according to fig.3

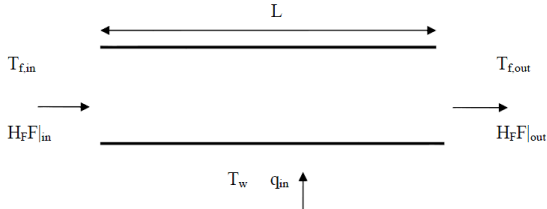


Figure 3. Furnace tube.

Unsteady state energy balance with the considered assumptions is as:

$$\frac{d(m_w C_{pw} T_w + m_f C_{pf} T_{f,m})}{dt} = q - (T_{f,out} - T_{f,in}) C_{pf} \dot{m}_f \quad (8)$$

Where,

$$T_{f,m} = \frac{(T_{f,in} + T_{f,out})}{2} \quad (9)$$

Supposing linear variation of gas temperature, tube exit temperature is equal to $T_{f,out}$ and $T_{f,m}$. Substituting equation (9) into (8) results in:

$$\frac{d(T_{f,out})}{dt} = \frac{q - (T_{f,out} - T_{f,in}) C_{pf} \dot{m}_f - \frac{m_f C_{pf}}{2} \frac{d(T_{f,in})}{dt}}{(m_w C_{pw} + \frac{m_f C_{pf}}{2})} \quad (10)$$

In the above equations q is the amount of heat absorbed by tubes. If the amount of heat generated by fuel is denoted by Q and the efficiency of the furnace by η , then:

$$q = \eta Q \quad (11)$$

D. Heat Exchanger Model:

Low order lumped parameter model of heat exchangers were used. Mathematical modeling plays an important role not only in designing and optimizing chemical engineering processes but also in studying the dynamic characteristics and controllability of existing equipment.

Fig. 4 depicts the thermal shell balance scheme on heat exchanger for developing the required model.

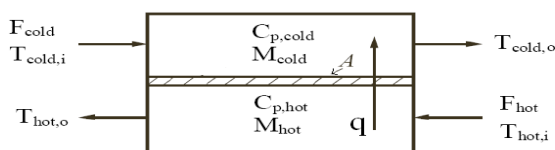


Figure 4. Heat Exchanger.

Assuming perfect mixing results in achieving a lumped parameter model for the heat exchanger, as below:

$$\frac{d(C_{p,cold} M_{cold} T_{cold,o})}{dt} = F_{cold} (H_{cold,i} - H_{cold,o}) - q \quad (12)$$

$$\frac{d(C_{p,hot} M_{hot} T_{hot,o})}{dt} = F_{hot} (H_{hot,i} - H_{hot,o}) - q \quad (13)$$

The heat transferred q is:

$$q = F U A \Delta T_m \quad (14)$$

Where, ΔT_m is logarithm of mean temperature difference.

$$\Delta T_m = \frac{(T_{hot,i} - T_{cold,o}) - (T_{hot,o} - T_{cold,i})}{\ln\left(\frac{T_{hot,i} - T_{cold,o}}{T_{hot,o} - T_{cold,i}}\right)} \quad (15)$$

E. Octane Number:

Octane number of the product from naphtha reforming unit can be expressed by concentrations as follows [14]:

$$RON = \sum_{r=1}^n b_r W_r \quad (16)$$

Where, b_r are coefficients and W_r are weight concentrations.

TABLE 2: GROUP DEFINITION AND REGRESSION COEFFICIENTS OF LINEAR RON MODEL DEVELOPED BY WALSH AND COWORKERS.

| Group no. | Group definition by GC elution times | Regression coefficient |
|-----------|--------------------------------------------------------------------------------|------------------------|
| 1 | Components eluting before <i>n</i> -butane | 103.9 |
| 2 | <i>n</i> -Butane | 88.1 |
| 3 | Components eluting between <i>n</i> -butane and isopentane | 144.3 |
| 4 | Isopentane | 84.0 |
| 5 | Components eluting between isopentane and <i>n</i> -pentane | 198.2 |
| 6 | <i>n</i> -Pentane | 67.9 |
| 7 | Components eluting between <i>n</i> -pentane and 2-methylpentane | 95.2 |
| 8 | 2- and 3-Methylpentane and components eluting between these | 86.6 |
| 9 | Components eluting between 3-methylpentane and <i>n</i> -hexane | 95.9 |
| 10 | <i>n</i> -Hexane | 20.9 |
| 11 | Components eluting between <i>n</i> -hexane and benzene | 94.9 |
| 12 | Benzene | 105.2 |
| 13 | Components eluting between benzene and 2-methylhexane | 113.6 |
| 14 | 2- and 3-Methylhexane and components eluting between these | 80.0 |
| 15 | Components eluting between 3-methylhexane and <i>n</i> -heptane | 97.8 |
| 16 | <i>n</i> -Heptane | -47.8 |
| 17 | Components eluting between <i>n</i> -heptane and toluene | 62.3 |
| 18 | Toluene | 113.9 |
| 19 | Components eluting between toluene and 2-methylheptane | 115.1 |
| 20 | 2- and 3-Methylheptane and components eluting between these | 81.7 |
| 21 | Components eluting between 3-methylheptane and <i>n</i> -octane | 109.7 |
| 22 | <i>n</i> -Octane | 10.5 |
| 23 | Components eluting between <i>n</i> -octane and ethylbenzene | 96.1 |
| 24 | Ethylbenzene | 122.6 |
| 25 | Components eluting between ethylbenzene and <i>p</i> -xylene | 45.4 |
| 26 | <i>p</i> -xylene + <i>m</i> -xylene | 102.0 |
| 27 | Components eluting between <i>m</i> -xylene and <i>o</i> -xylene | 73.3 |
| 28 | <i>o</i> -Xylene | 123.6 |
| 29 | Components eluting after <i>o</i> -xylene up to and including <i>n</i> -nonane | 35.0 |
| 30 | Components eluting between <i>n</i> -nonane and <i>n</i> -decane | 112.0 |
| 31 | <i>n</i> -Decane and components eluting after <i>n</i> -decane | 85.6 |

III. SIMULATION

Level-1 M-files of S-function in MATLAB software are used in this paper for simulating the above equations. Distribution of nodes in the space of reactor plays an important role in converging to the solution when solving the equations. Nodes in beginning of reactor are very close together according to Fig. 5.

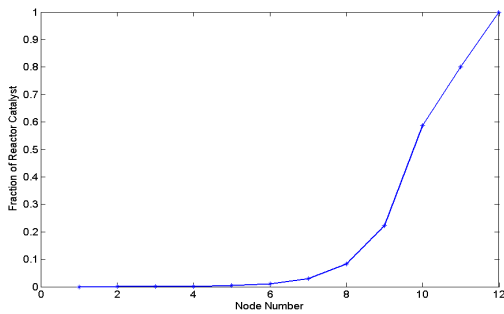


Figure 5. Node distribution in reactor length.

Derivative terms in the right hand side of partial differential equations are fitted by second order polynomial.

$$y = cx^2 + bx + a \quad (17)$$

Slope is calculated from the equation:

$$\frac{dy}{dx} = 2cx + b \quad (18)$$

Constants b and c can be calculated using the values of three consecutive nodes.

Fig. 6 shows a flow diagram of the system simulated via MATLAB SIMULINK.

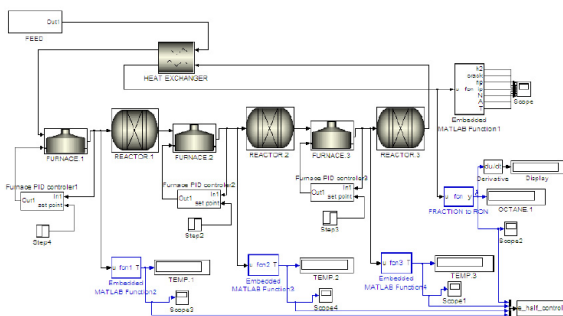


Figure 6. Dynamic model and simulation of model by MATLAB software.

In the SIMULINK mode all variables can be plotted versus time. The Solver type used in simulation is ode23tb with variable steps.

IV. RESULTS AND DISCUSSION

Results of simulated model are compared with experimental data obtained from the operation data sheets of a refinery plant in Iran and are shown in Fig. 7. In order to validate the dynamic model, output temperatures of the reactors for input temperatures of three degrees centigrade are compared with the data of a refinery in Iran. Plant data are collected at every 600 seconds. The results of simulation and comparison are shown in figures 7, 8 and 9.

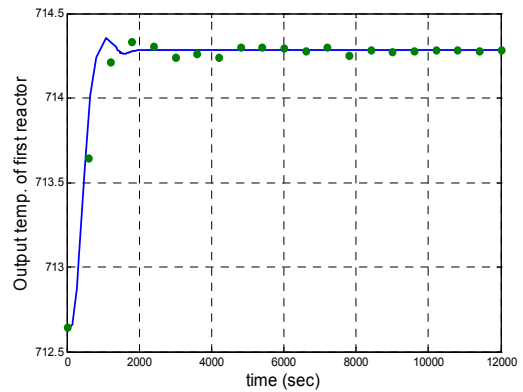


Figure 7. Comparison of plant data with simulated model for 3 o C temperature rise in reactor 1.

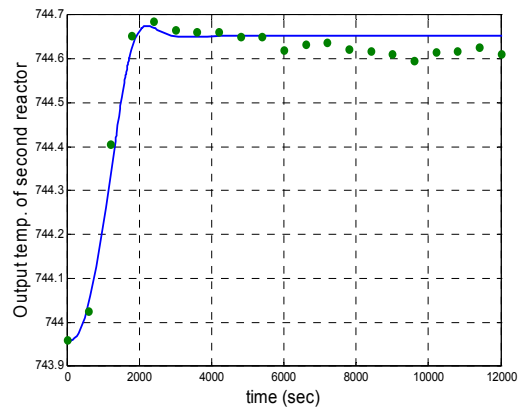


Figure 8. Comparison of plant data with simulated model for 3 o C temperature rise in reactor 2.

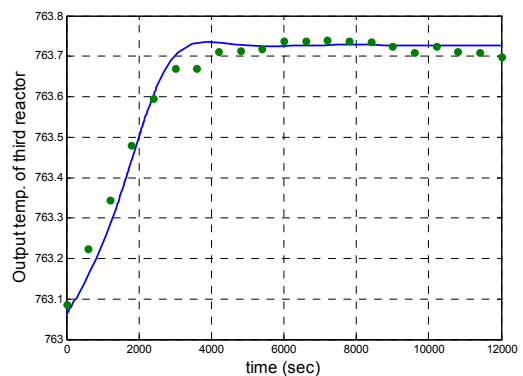


Figure 9. Comparison of plant data with simulated model for 3 o C temperature rise in reactor 3.

SATISFACTORY FITTING BETWEEN PLANT AND MODEL IS DETECTED FROM THE FIGURES.

V. CONCLUSION

In this paper, simulation of the dynamic model of the catalytic naphtha reformer process by MATLAB software is presented. The kinetic parameters of model are based on the steady state condition and are obtained from a commercial plant data furnished by a domestic petroleum refinery. This dynamic model is in form of partial differential equations. The nonlinear model of the system was solved numerically by MATLAB software.

The simulation results reveals of satisfactory fitness between data and the model.

NOMENCLATURE

| | |
|---------------------------------|-------------------------------|
| A_c | Catalyst bed area |
| c_i (kmol / m ³) | Particle i mole concentration |
| d_p (m) | Catalyst diameter |
| E_{A_i} | Activation energy |
| G (kg / m ² .s) | Total mass flux |
| ϵ | Porosity of catalyst bed |
| μ (pa.s) | Viscosity |
| r_i (kmol / kg cat.s) | Reaction Rate |
| R | Gas constant |
| ρ_s (kg / m ³) | Density of catalyst particle |
| ρ_f (kg / m ³) | Fluid Density |
| Ω (m ²) | Catalyst bed Area |
| M_{av} (kg / kmol) | Average molecular weight |

APPENDIX A

Mass balance equation for element of catalyst weight in a plug flow reactor is:

$$F_{i,w} - F_{i,w+dw} + \sum_{j=1}^{n_r} \gamma_{i,j} r_j dw = \frac{d(n_i)}{dt} = \frac{d(c_i)}{dt} \frac{\epsilon}{\rho_b} dw \quad (19)$$

In the above equation n_i is as bellow:

$$n_i = c_i \frac{\epsilon}{\rho_b} dw \quad (20)$$

And in final step the following equation is attained:

$$-\frac{dF_i}{dw} + \sum_{j=1}^{n_r} \gamma_{i,j} r_j = \frac{\epsilon}{\rho_b} \frac{d(c_i)}{dt} \quad (21)$$

APPENDIX B

Energy balance equation for an element of catalyst weight in a plug flow reactor is:

$$\sum_{i=1}^{n_c} F_i H_i \Big|_w - \sum_{i=1}^{n_c} F_i H_i \Big|_{w+dw} = \frac{dE_{sys}}{dt} \quad (22)$$

Differential form of the above equation is in the form:

$$-\frac{d(\sum_{i=1}^{n_c} F_i H_i)}{dw} dw = \frac{dE_{sys}}{dt} \quad (23)$$

The following equation is attained by expansion of the left hand side of the above equation:

$$-\frac{d(\sum_{i=1}^{n_c} F_i H_i)}{dw} dw = -(\sum_{i=1}^{n_c} F_i \frac{dH_i}{dw}) dw - (\sum_{i=1}^{n_c} H_i \frac{dF_i}{dw}) dw \quad (24)$$

Internal energy is related to enthalpy and by expansion of the right hand side of equation (20) we have:

$$\begin{aligned} \frac{dE_{sys}}{dt} &= \frac{d(E_{cata} + \sum_{i=1}^{n_c} n_i (H_i - PV_i))}{dt} \\ &= \frac{dE_{cata}}{dt} dw + \sum_{i=1}^{n_c} n_i \frac{dH_i}{dt} \\ &\quad + \sum_{i=1}^{n_c} H_i \frac{dn_i}{dt} - \frac{d(PV)}{dt} \\ &= \frac{dE_{cata}}{dt} dw + \sum_{i=1}^{n_c} n_i \frac{dH_i}{dt} \\ &\quad + \sum_{i=1}^{n_c} H_i \left(\frac{\epsilon dw}{\rho_b} \right) \frac{dc_i}{dt} - \frac{d(PV)}{dt} \end{aligned} \quad (25)$$

Where V is the volume of catalyst element upon which the balance is performed.

$$V = \frac{\epsilon}{\rho_b} dw \quad (26)$$

n_i is the number of i'th lump mole in the element with dw of catalyst weight.

By equations (19) and (23) the following equation is obtained:

$$\frac{dE_{sys}}{dt} = \frac{dE_{cata}}{dt} dw + \sum_{i=1}^{n_c} n_i \frac{dH_i}{dt} + \quad (27)$$

$$\sum_{i=1}^{n_c} H_i \left(-\frac{dF_i}{dw} + \sum_{j=1}^{n_r} \gamma_{i,j} r_j \right) dw - \frac{d(P)}{dt} \frac{\epsilon}{\rho_b} dw$$

By equation (7), (20), (23), (25) and (27), and by ignoring pressure effects, we reach to the following equation:

$$\begin{aligned} -\left(\sum_{i=1}^{n_c} F_i C_{pi} \frac{dT}{dw} \right) &= C_{pcata} \frac{dT}{dt} + \frac{\epsilon}{\rho_b} \sum_{i=1}^{n_c} c_i C_{pi} \frac{dT}{dt} \\ &\quad + \sum_{j=1}^{n_r} r_j \left(\sum_{i=1}^{n_c} H_i \gamma_{i,j} \right) \end{aligned} \quad (28)$$

And the resulted final equation is:

$$\frac{dT}{dt} = \frac{-\left(\sum_{i=1}^{n_c} F_i C_{pi} \right) \frac{dT}{dw} - \sum_{j=1}^{n_r} r_j \left(\sum_{i=1}^{n_c} H_i \gamma_{i,j} \right)}{\left(C_{pcata} + \frac{\epsilon}{\rho_b} \sum_{i=1}^{n_c} c_i C_{pi} \right)} \quad (29)$$

REFERENCES

- [1] Smith, R.B. (1959). Kinetic analysis of naphtha reforming with platinum catalyst. Chem. Eng. Prog. 55, 6, 76.
- [2] Kmak, W.S., Stuckey, A.N. (1973). Powerforming process studies with a kinetic simulation model. AIChE National Meeting, New Orleans, March, Paper No. 56a.
- [3] Froment, G.F. (1987). The Kinetic of Complex Catalytic Reactions. Chem. Eng. Sci., 42, 5, 1073.

- [4] Ramage, M.P., Graiani, K.R., Krambeck, F.I. (1980). Development of Mobil's kinetic reforming model. *Chem. Eng. Sci.*, 35, 1, 41
- [5] Jorge Ancheyta-Luarez, Eduardo Villafuene-Macias. (2000). Kinetic Modeling of Naphtha Catalytic Reforming Reactions. *Energy & Fuels*, 14, 5, 1032.
- [6] Taskar, U., Riggs, J.B. (1997). Modeling and optimization of a semi-regenerative catalytic naphtha reformer. *AIChE*, 43, 3, 740.
- [7] Hu, Y., Su, H., Chu, J. (2003). Modeling, Simulation and Optimization of Commercial Naphtha Catalytic Reforming Process. *Proceedings of the 42nd IEEE Conference on Decision and Control*, 6206-6211, Dec. 9-12, Hawaii, USA.
- [8] Rahimpour, M.R., Esmaili, S., Bagheri, G.N.A., "Kinetic and deactivation model for industrial catalytic naphtha reforming", *Iran. J. Sci. Tech., Trans. B: Tech.*, 27, 279-290 (2003).
- [9] Hu, Y.Y., Su, H.Y., Chu, J., "The research summarize of catalytic reforming unit simulation", *Contr. Instrum. Chem. Ind.* 2, 9 (2), 19-23 (2002). (In Chinese)
- [10] H. M. Arani, M. Shirvani, K. Safdarian and E. Dorostkar, "Lumping procedure for a kinetic model of catalytic naphtha reforming" *Braz. J. Chem. Eng.* vol.26 no.4 Oct./Dec. 2009
- [11] HOU Weifen, SU Hongye, HU Yongyou, CHU Jian, Zhejiang University, "Modeling, Simulation and Optimization of a Whole Industrial Catalytic Naphtha Reforming Process on Aspen Plus Platform", *Chinese J. Chem. Eng.*, 14(5) 584-591 (2006).
- [12] M. R. Rahimpour, "Operability of an Industrial Catalytic Naphtha Reformer in the Presence of Catalyst Deactivation", *Chem. Eng. Technol.*, 29, No. 5, (2006).
- [13] Yongyou Hu, Weihua Xu, Hongye Su, Jian Chu, Zhejiang university, "Modeling, Simulation and Optimization of Commercial Naphtha Catalytic Reforming Process", *IEEE*, (2004).
- [14] George J. Fintos, Abdullah M. Aitan, "Catalytic naphtha reforming, second edition, revised and expanded", MARCELD EKKER, INC, (2004).
- [15] Yongyou Hu, Weihua Xu, Hongye Su, Jian Chu, Zhejiang university, "A Dynamic Model for Naphtha Catalytic Reformers", *IEEE*, Taiwan, September 2-4, 2004
- [16] R.M. Ansari, M.O. Tade, "Constrained nonlinear multivariable control of a catalytic reforming process", *Control Engineering Practice* 6 (1998) 695-706.
- [17] Anderson, P.C.; Sharkey, J.M.; Walsh, R.P. *J. Inst. Petr.* 1972, 58 (560), 83.